# Modeling the pulse shape of Q-switched lasers to account for terminal-level relaxation

Zeng Qin-Yong(曾钦勇)[a)b)†], Wan Yong(万 勇)[a)b)], Xiong Ji-Chuan(熊吉川)[b)], and Zhu Da-Yong(朱大勇)[a)]

[a)] *School of Optoelectronic Information, University of Electronic Science and Technology of China, Chengdu* 610054, *China*
[b)] *Southwest Institute of Technical Physics, Chengdu* 610041, *China*

(Received 20 May 2010; revised manuscript received 15 October 2010)

To account for the effect of lower-level relaxation, we have derived a characteristic equation for describing the laser pulse from the modified rate equations for Q-switched lasers. The pulse temporal profile is related to the ratio of the lower-level lifetime to the cavity lifetime and the number of times the population inversion density is above the threshold. By solving the coupled rate equations numerically, the effect of terminal-level lifetime on pulse temporal behaviour is analysed. The mode is applied to the case of a diode-pumped Nd:YAG laser that is passively Q-switched by a $Cr^{4+}$:YAG absorber. Theoretical results show good agreement with the experiments.

**Keywords:** solid state laser, passive Q-switch, $Cr^{4+}$:YAG absorber
**PACS:** 42.55.Ah, 42.60.Gd **DOI:** 10.1088/1674-1056/20/3/034204

## 1. Introduction

Diode-pumped solid-state Q-switched lasers have been widely used in the fields of remote sensing, information storage, telecommunications, medicine, etc., and much research regarding their modeling and optimisation has been published.[1−6] Previous studies have shown that the pulse temporal profile of Q-switched lasers is usually asymmetric, with unequal rising and falling edges.[7,8] In some applications, accurate knowledge of the pulse shape is useful. For example, applications in telecommunications may require details of the temporal profile of pulse trains from the transmitter in order to design a proper receiver. Initial studies have described the pulse shape for different losses and cross sections in both actively and passively Q-switched lasers.[9−12] Siegman[13] related the pulse shape to the ratio of population inversion density at the onset of Q-switch to that at threshold by solving the rate equations numerically. Liu *et al.*[14] developed a general method to analyse the pulse shape of a Q-switched laser and showed that the pulse shape is asymmetric, with a fast leading edge and a slow trailing edge, in a $Cr^{4+}$: YAG Q-switched laser. However, the above analysis has not accounted for the effect of the finite lower-level lifetime in the Nd:YAG, which has a significant effect on pulse shape. In Ref. [15], it was assumed that the lower-level lifetime is short compared to the pulse duration and laser cavity lifetime, while the reported measurements of the $4I_{11/2}$ level lifetime $\tau_2$ range from as short as 10 ns to as long as 1 $\mu$s. In a Q-switched Nd:YAG laser with pulse-width of the order of tens of ns, even for the smallest value of $\tau_2$ reported, the assumption may lead to substantial inaccuracy. Tso[16] has reported on a study of the effect of a finite $\tau_2$ on the extraction efficiency and pulse shape in Q-switched Nd:YAG lasers, but the detailed symmetric property of the laser pulse was not given in Ref. [16]. Degnan *et al.*[15] discussed the effects of thermalisation in addition to lower-level relaxation on Q-switched laser properties and showed that the pulse shape will be affected by either process if the pulse duration is of the order of the thermalisation time or lower-level lifetime.

In this paper, from the coupled rate equations including the lower-level lifetime in Nd:YAG, a general equation describing the temporal behaviour of laser pulse for both actively and passively Q-switched lasers is derived. This equation extends Liu's result[14] and enables treatment of the more general case when pulse duration is of the order of terminal-level lifetime. Using the concept of symmetry factor, the effect of lower manifold lifetime on pulse shape is investigated quantitatively, and the results are compared with those in the case of infinitely fast lower-level relaxation previously assumed. The modified model is applied to a

†Corresponding author. E-mail: zengqy209@163.com
© 2011 Chinese Physical Society and IOP Publishing Ltd

Nd:YAG laser operated at 1064 nm, and good agreement is shown between theoretical results and experiments.

## 2. General model of equations for Q-switched lasers

We begin with the rate equations of the populations in upper and lower manifolds for a passively Q-switched laser including the effect of lower-level relaxation,

$$\frac{\mathrm{d}n_3}{\mathrm{d}t} = -f_3 c\sigma n\phi, \tag{1a}$$

$$\frac{\mathrm{d}n_2}{\mathrm{d}t} = f_2 c\sigma n\phi - \frac{n_2}{\tau_2}, \tag{1b}$$

$$n = n_3 - n_2. \tag{2}$$

Here, $f_3$ and $f_2$ are the equilibrium fractional Boltzmann populations of the upper and lower laser levels within their respective multiplets; $t$ is time, $\sigma$ is the stimulated emission cross section, $\tau_2$ is the lifetime of the lower- level multiplets, $\Phi$ is the cavity photon density, $c$ is the speed of light, $n_3$ and $n_2$ are the population densities of the upper and lower laser level respectively. Taking the Fourier transform of Eqs. (1) and (2), and solving for the Fourier transforms of the inversion density yield

$$\overline{n} = -\overline{\gamma} c\sigma \overline{n\phi}, \tag{3}$$

where $\overline{\gamma}$ is the Fourier transform of the inversion reduction factor $\gamma$. In a four-level system or a three-level system, disregarding the thermalisation time or lower leve relaxation, the 'inversion reduction factor' $\gamma$ is typically a constant equal to $f_3 + f_2$. Thus, we can perform the inverse Fourier transform of Eq. (3) and obtain

$$\frac{\mathrm{d}n}{\mathrm{d}t} = -\gamma c\sigma n\varphi. \tag{4}$$

This is the regular form of rate equation describing the population inversion density in a gain medium. However, when the lower-level relaxation time $\tau_2$ is of the order of pulse-width, the effect of finite lower-level lifetime should be included in rate equations as Eq. (1b), $\gamma$ becomes time-dependent and its Fourier transform can be expressed as

$$\overline{\gamma(\omega)} = \frac{f_3}{\mathrm{i}\omega} + \frac{f_2\tau_2}{1 + \mathrm{i}\omega\tau_2}. \tag{5}$$

Thus, the inversion reduction factor $\gamma$ is

$$\gamma(t) = f_3 + f_2\,\mathrm{e}^{-t/\tau_2}. \tag{6}$$

For convenience of numerical modeling, we substitute Eq. (6) directly into Eq. (4) to obtain the rate equation for population inversion density,

$$\frac{\mathrm{d}n}{\mathrm{d}t} = -\gamma(t)\, c\sigma n\varphi. \tag{7}$$

In this process, the inversion reduction factor $\gamma$ is treated independently from $n(t)$ and $\varphi(t)$, thus a result can be obtained much simpler than the exact but complex expression with convolution of $n(t)$, $\varphi(t)$, and $\gamma(t)$ as in Ref. [15].

In Nd:YAG, the energy gap between the terminal and ground multiplets is about 30 times that of the typical Stark splitting within these multiplets.[17] Thus, according to the energy gap law, the thermalisation within the upper and lower manifolds should be a much faster process than the terminal-level relaxation. Hence, only the terminal-level lifetime, which is on the order of pulse-width, needs to be considered. The coupled rate equations for a passively Q-switched laser can be written as

$$\frac{\mathrm{d}\phi}{\mathrm{d}t} = \frac{\phi}{t_\mathrm{r}}\Big[2\sigma nl - 2\sigma_{13}n_{\mathrm{s}1}l_\mathrm{s} - 2\sigma_{24}(n_{\mathrm{s}0} - n_{\mathrm{s}1})\,l_\mathrm{s} - \ln\left(\frac{1}{R}\right) - L\Big], \tag{8}$$

$$\frac{\mathrm{d}n}{\mathrm{d}t} = -\gamma(t)\, c\sigma n\phi, \tag{9}$$

$$\frac{\mathrm{d}n_{\mathrm{s}1}}{\mathrm{d}t} = -\frac{A_\mathrm{g}}{A_\mathrm{s}} c\sigma_{13} n_{\mathrm{s}1}\phi. \tag{10}$$

Here $l$ is the length of the gain medium, $t_\mathrm{r}$ is the cavity round-trip time, and $L$ is the fractional cavity loss per round-trip; $\Phi$ is the intra-cavity photon density, $n$ is the average instantaneous population inversion density in the active laser medium with effective length of $l$, $R$ is the reflectance of the output coupler; $\sigma_{13}$ and $\sigma_{24}$ are the ground-and excited-state absorption cross sections of the absorber, $n_{\mathrm{s}1}$ is the population density of saturable absorber in the ground state, and $n_{\mathrm{s}0}$ is the total density of the absorber with absorption length of $l$s. $A_\mathrm{g}$ and $A_\mathrm{s}$ are diameters of the beam spots in laser medium and absorber, respectively.

Dividing Eq. (9) by Eq. (10) and integrating the result yields the relationship between $n_{\mathrm{s}1}$ and $n_{\mathrm{s}0}$, i.e.,

$$\frac{n_{\mathrm{s}1}}{n_{\mathrm{s}0}} = \left(\frac{n}{n_\mathrm{i}}\right)^{\alpha}, \tag{11}$$

where $n_\mathrm{i}$ is the initial population inversion density when the pulse begins, and $\alpha$ is defined as

$$\alpha = \frac{\sigma_{13}A_\mathrm{g}}{\gamma(t)\,\sigma A_\mathrm{s}}. \tag{12}$$

Since $\alpha$ is the parameter describing the behaviour of the switcher, it is only determined by the performance of the Q-switching at the onset of the pulse. If the Q-switching process is fast enough, we can assume that the property of the saturable absorber remains the same as that at the beginning of Q-switching, when $t = 0$. Hence $\alpha$ is a constant defined as the following equation when $\gamma(0) = f_3 + f_2$,

$$\alpha = \frac{\sigma_{13} A_{\mathrm{g}}}{(f_3 + f_2)\,\sigma A_{\mathrm{s}}}. \tag{13}$$

To simplify the rate equations, we define the following parameters

$$\ln\left(\frac{1}{T_0^2}\right) = 2\sigma_{13} n_{\mathrm{s}0} l_{\mathrm{s}}, \tag{14}$$

$$z = \frac{n(t)}{n_{\mathrm{i}}}, \tag{15}$$

$$\tau_{\mathrm{c}} = \frac{t_{\mathrm{r}}}{\ln(1/R) + L}, \tag{16}$$

$$x = \frac{(1-\delta)\ln(1/R)}{2\sigma n_{\mathrm{i}} l}, \tag{17}$$

$$y = \frac{(1-\delta)\ln\left(1/T_0^2\right)}{2\sigma n_{\mathrm{i}} l}, \tag{18}$$

where $T_0$ is the initial transmission of saturable absorber and $z$ is the ratio of the population inversion density at any instant to the initial inversion density at the onset of Q-switching. Dividing Eq. (8) by Eq. (9) and substituting Eqs. (12)–(17) into the result yields

$$\phi(z) = \frac{\ln_i}{\gamma l'}\left[1 - z - \frac{y}{\alpha}\left(1 - z^{\alpha}\right) + (1-y)\ln z\right], \tag{19}$$

$$\frac{\mathrm{d}\varphi}{\mathrm{d}z} = -\frac{l}{\gamma l'}\left[1 - y z^{\alpha-1} - (1-y)\, z^{-1}\right]. \tag{20}$$

If $n_{\mathrm{p}}$ and $n_{\mathrm{f}}$ are the population inversion densities at which the maximum intra-cavity photon density is reached, and when the photon density drops to zero at the pulse final state, the relation between $n_{\mathrm{p}}$ and $n_{\mathrm{f}}(z_{\mathrm{p}} = n_{\mathrm{p}}/n_{\mathrm{i}},\ z_{\mathrm{f}} = n_{\mathrm{f}}/n_{\mathrm{i}})$ are

$$1 - z_{\mathrm{f}} - \frac{y}{\alpha}\left(1 - z_{\mathrm{f}}^{\alpha}\right) + (1-y)\ln(z_{\mathrm{f}}) = 0, \tag{21}$$

$$1 - y z_{\mathrm{p}}^{\alpha-1} - (1-y)\, z_{\mathrm{p}}^{-1} = 0; \tag{22}$$

and the instantaneous power $P(t)$ is

$$P(t) = \frac{h\nu A_{\mathrm{g}} n_{\mathrm{i}} l \ln(1/R)}{t_{\mathrm{r}}} \cdot \frac{1}{\gamma} \times \left[1 - z - \frac{y}{\alpha}\left(1 - z^{\alpha}\right) + (1-y)\ln z\right]. \tag{23}$$

Define $p(t)$ as

$$p(t) = \frac{1}{\gamma}\left[1 - z - \frac{y}{\alpha}\left(1 - z^{\alpha}\right) + (1-y)\ln z\right]. \tag{24}$$

At the moments $t_1$ and $t_2$, $\gamma_1$ and $\gamma_2$ are the values of $\gamma(t)$ determined by Eq. (7), the normalised population inversion densities are $z_1 = n(t_1)/n_{\mathrm{i}}$ and $z_2 = n(t_2)/n_{\mathrm{i}}$. As shown in Fig. 1, $p_{\mathrm{p}}$ is the peak power and $mp_{\mathrm{p}}$ $(0 < m < 1)$ is the output power at times $t_1$ and $t_2$; $\gamma_{\mathrm{p}}$ is the value of $\gamma(t)$ at the time of peak power $t_{\mathrm{p}}$, then

$$mp_{\mathrm{p}} = \frac{1}{\gamma(t)}\left[1 - z_{1,2} - \frac{y}{\alpha}\left(1 - z_{1,2}^{\alpha}\right) + (1-y)\ln(z_{1,2})\right], \tag{25}$$

where

$$p_{\mathrm{p}} = \frac{1}{\gamma_{\mathrm{p}}}\left[(1 - z_{\mathrm{p}})\left(1 - \frac{1}{\alpha}\right) + (1-y)\ln(z_{\mathrm{p}})\right]. \tag{26}$$

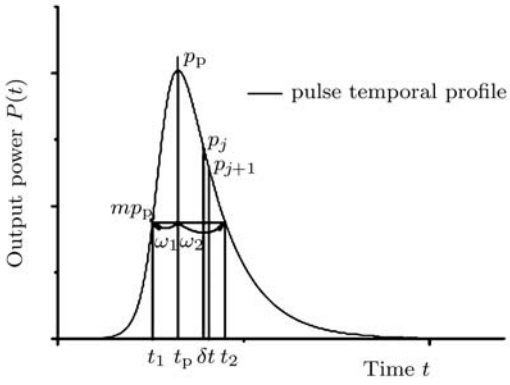



**Fig. 1.** Definition of parameters for pulse symmetry calculation.

From Eqs. (21), (25), and (26), the relation between $z_1$ and $z_2$ is

$$\begin{aligned} & f(z_{\mathrm{p}}, m) \\ &= m(1 - z_{\mathrm{p}})\left(1 - \frac{1}{\alpha}\right) \\ &\quad + \frac{z_{\mathrm{p}} - z_{\mathrm{p}}^{\alpha}}{1 - z_z^{\alpha}}\left(\frac{m}{\gamma_{\mathrm{p}}}\ln z_{\mathrm{p}} - \frac{1}{\gamma_{1,2}}\ln z_{1,2}\right) \\ &\quad - \frac{1}{\gamma_{1,2}}\left(1 - z_{1,2} - \frac{1 - z_{\mathrm{p}}}{1 - z_{\mathrm{p}}^{\alpha}} \cdot \frac{1 - z_{1,2}^{\alpha}}{\alpha}\right) \\ &= 0. \end{aligned} \tag{27}$$

If $\gamma$ equals 1, this characteristic equation has exactly the same form of Eq. 32 in Ref. [14]. Specifically, this extended version of Liu's result enables the treatment of the more general case when pulse duration is on the order of the terminal-level lifetime. In this characteristic equation, the reciprocal of variable $z_{\mathrm{p}}$ denotes the number of times of the initial population inversion above the dynamic threshold, which has the same meaning as $r$ in Ref. [16]. Integrating Eq. (9)

and substituting Eq. (19) into the result, we obtain the relation between $t$ and $z$

$$t = -\frac{l'}{c\sigma n_{\mathrm{i}} l} \times \int_1^z \frac{1}{z \cdot \left[1 - z - \dfrac{y}{\alpha}\left(1 - z^{\alpha}\right) + (1 - y)\ln z\right]} \mathrm{d}z. \tag{28}$$

Together with Eq. (28), we can find two degenerate roots of Eq. (27), $z_1$ and $z_2$, for any given value of $m$, $z_{\mathrm{p}}$, and $\tau_2$.

Now, we can analyse the effect of the terminal-level lifetime on the pulse shape, using the symmetry factors defined by Liu in Ref. [14]

$$\varepsilon_{\mathrm{e}}\left(z_{\mathrm{p}}, m\right) = \frac{e_{\mathrm{p2}}}{e_{1\mathrm{p}}}. \tag{29}$$

And

$$\varepsilon_{\mathrm{t}}\left(z_{\mathrm{p}}, m\right) = \frac{\omega_2\left(z_{\mathrm{p}}, m\right)}{\omega_1\left(z_{\mathrm{p}}, m\right)}, \tag{30}$$

where $\omega_1(z_{\mathrm{p}}, m)$ and $\omega_2(z_{\mathrm{p}}, m)$ are the time intervals from $t_1$ to $t_{\mathrm{p}}$ and $t_{\mathrm{p}}$ to $t_2$; $e_{1\mathrm{p}}$ and $e_{\mathrm{p2}}$ are the normalised energies extracted in the two time intervals, then we have

$$\omega_1\left(z_{\mathrm{t}}, m\right) = t_{\mathrm{p}} - t_1, \tag{31}$$

$$\omega_2\left(z_{\mathrm{t}}, m\right) = t_2 - t_{\mathrm{p}}. \tag{32}$$

Using a finite difference approximation to Eq. (24), we obtain the expression for $e_{1\mathrm{p}}$ and $e_{\mathrm{p2}}$

$$e_{1\mathrm{p}}\left(z_{\mathrm{p}}, m\right) = \sum_{j=0}^{N} \frac{p_j + p_{j+1}}{2} \cdot \delta t, \tag{33}$$

$$e_{\mathrm{p2}}\left(z_{\mathrm{p}}, m\right) = \sum_{j=0}^{M} \frac{p_j + p_{j+1}}{2} \cdot \delta t, \tag{34}$$

where $\delta t$ is the temporal step size, and $N$ and $M$ are numbers of steps at the rising and falling edges, respectively. Using Eqs. (29) and (30) together with the characteristic equation (27), the pulse symmetry from the viewpoint of energy can be described. Furthermore, the pulse temporal profile can be depicted using Eqs. (27) and (28) for any given $z_{\mathrm{p}}$ and $\tau_2$.

Figure 2 shows the normalised output power as a function of time for different values of $z_{\mathrm{p}}$ and $\tau_2$. For the same value of $z_{\mathrm{p}}$, a larger value of $\tau_2$ leads to relatively longer falling edge. This effect can be depicted quantitatively with $\varepsilon_{\mathrm{e}}(z_{\mathrm{p}}, m)$ and $\varepsilon_{\mathrm{t}}(z_{\mathrm{p}}, m)$ as functions of $z_{\mathrm{p}}$ for different $\tau_2$.

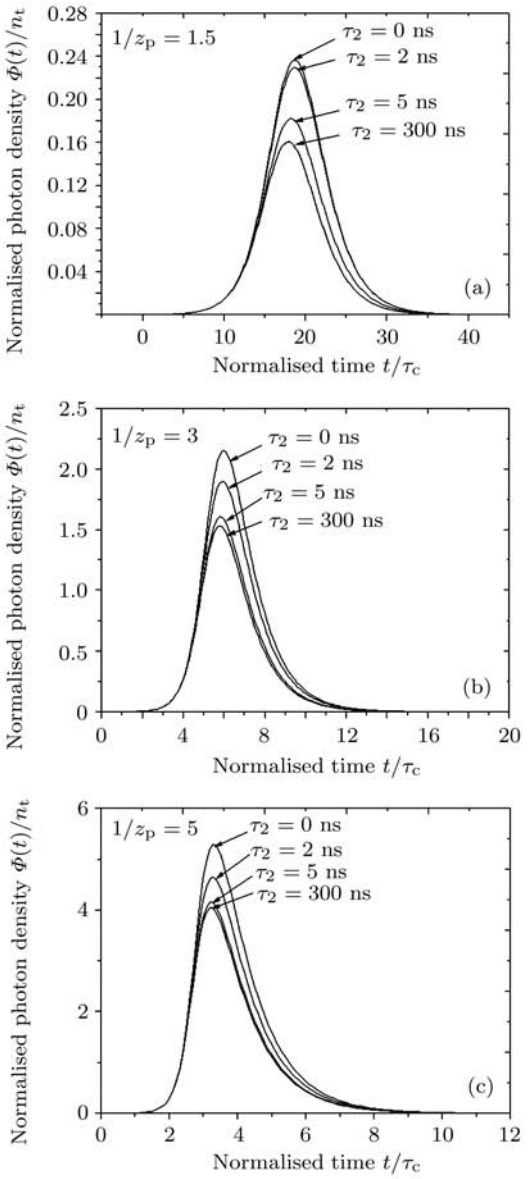



**Fig. 2.** Normalised photon density $\phi(t)/n_{\mathrm{t}}$ versus normalised time $t/\tau_{\mathrm{c}}$ for different values of $z_{\mathrm{p}}$ and $\tau_2$, where $\tau_{\mathrm{c}}$ is the cavity lifetime. $1/z_{\mathrm{p}}$ denotes the number of times the initial population inversion above the dynamic threshold. (a) $1/z_{\mathrm{p}} = 2$, (b) $1/z_{\mathrm{p}} = 3$, (c) $1/z_{\mathrm{p}} = 5$.

Figure 3 shows $\varepsilon_{\mathrm{e}}(z_{\mathrm{p}}, 05)$ and $\varepsilon_{\mathrm{t}}(z_{\mathrm{p}}, 05)$ versus $1/z_{\mathrm{p}}$ for different values of $\tau_2$. They describe the pulse waveform symmetries at half maximum in terms of energy and time interval, respectively. From Fig. 3, it is seen that, as $1/z_{\mathrm{p}}$ increases, the pulse symmetry factors in terms of energy and time interval both increase. For longer lower- level lifetime $\tau_2$, the symmetry factors are smaller for specific value of $z_{\mathrm{p}}$. When the terminal-level lifetime is large enough, e.g., $\tau_2 =$ 30 ns, the pulse symmetry becomes the same as that at $\tau_2 = 300$ ns, which means very slow relaxation in the lower level. This results from the fact that, if the

lower- level lifetime is of a value comparable to the pulse-width, the terminal level will be populated during the pulse duration instead of being depopulated rapidly as assumed in the case of infinite fast lower-level relaxation. Thus the population inversion will decrease faster and result in a shorter pulse falling edge. Then the pulse symmetry factor will be smaller for longer lower-level lifetime, noticing that the pulse rising edge is not effected substantially by the value of $\tau_2$.[15]

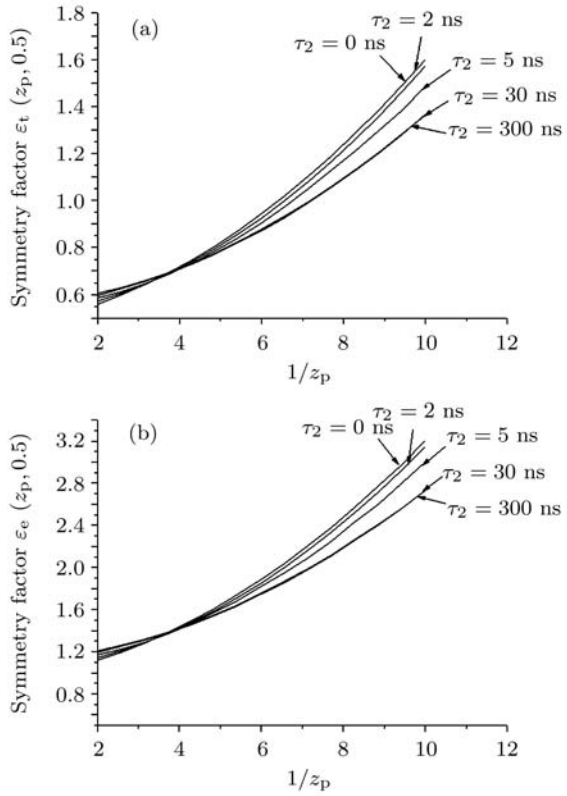



**Fig. 3.** Variation in the pulse symmetry factors $\varepsilon_t(z_p, 05)$ (a) and $\varepsilon_e(z_p, 05)$ (b) with $1/z_p$ for different values of terminal-level lifetime $\tau_2$.

## 3. Example

As an example for experimental confirmation of the above theoretical modeling, we use Nd:YAG as a gain medium of length $l = 5$ mm but coupled to a $Cr^{+4}$:YAG saturable absorber of length 1 mm. The laser rod is of a diameter of 6 mm and end-pumped through a fibre by a laser diode of 30 W nominal power at a wavelength of 808 nm. The laser rod is anti-reflection (AR) coated at wavelength 808 nm and high-reflection (HR) coated at 1064 nm for the surface facing the pumping end. The other end of the rod is AR coated at 1064 nm. The saturable absorber, with small signal transmission of 70%, is AR coated at 1064 nm on both sides. The output coupling reflectivity is given as $R = 85\%$.

Now we return to our theoretical modeling of the pulse temporal behaviour expressed in our implicit solution (see Eqs. (27) and (28)). Figure 4 shows the simulated pulse shape, solid curve and that compared to the experimental results shown as dashed curve. From Fig. 4, it is seen that the experimental data remain within 10% of our implicit solution for $\tau_2 = 30$ ns, $z_p = 2.5$. Inexactly valued $\tau_2$ and $z_p$ in simulation and measurement inaccuracy in experiment together bring the tiny diversity between curve (a) and curve (b). The value of $z_p$ is determined by the experiment setup. The estimation of $\tau_2 = 30$ ns is comparable to earlier measurements or computations in various crystals and glasses (5 ns $< \tau_2 <$ 300 ns).[15,17−19]

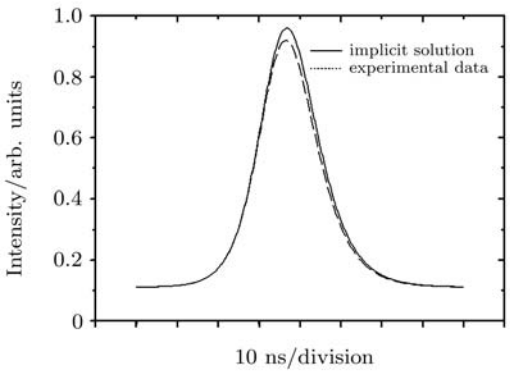



**Fig. 4.** Pulse shape as a function of time. (Experimental: dashed curve; simulation: solid curve)

## 4. Conclusion

In conclusion, we have demonstrated a general pulse shape model for Q-switched lasers to account for the effect of lower-level relaxation. We developed characteristic equations describing the pulse shape of Q-switched lasers, and some calculated curves were given to illustrate the effect of lower-level relaxation on the properties of pulse symmetry. With these general characteristic equations, one can easily estimate the pulse temporal behaviour and calculate the symmetry properties in Q-switched lasers. The theoretical modeling is compared with the experimental results and good agreement is shown.

# References


[1] Degnan J J 1995 *IEEE J. Quantum Electron.* **QE-31** 1890
[2] Degnan J J 1989 *IEEE J. Quantum Electron.* **QE-25** 214
[3] Zayhowski J J and Kelley P L 1991 *IEEE J. Quantum Electron.* **QE-27** 2220
[4] Zhang X, Zhao S, Wang Q, Liu Y and Wang J 1994 *IEEE J. Quantum Electron.* **QE-30** 905
[5] Xiao G and Bass M 1997 *IEEE J. Quantum Electron.* **QE-33** 41
[6] Zhang X, Zhao S, Wang Q, Zhang Q, Sun L and Zhang S 1997 *IEEE J. Quantum Electron.* **QE-33** 2286
[7] Zhao S, Zhang X, Zheng J, Chen L, Cheng Z and Cheng H 2002 *Opt. Eng.* **41** 559
[8] Li Z, Xiong Z, Moore N, Lim G C, Huang W L and Huang D X 2004 *Opt. Commun.* **237** 411
[9] Wegnar W G and Lengel B A 1963 *J. Appl. Phys.* **42** 2040
[10] Szabo A and Stein R A 1965 *J. Appl. Phys.* **36** 1562
[11] Erickson L E and Szabo A 1966 *J. Appl. Phys.* **37** 4953
[12] Erickson L E and Szabo A 1967 *J. Appl. Phys.* **38** 2540
[13] Siegman A E 1986 *Lasers* (Oxford: Oxford Unversity Press) p25
[14] Liu J, Shen D, Tam S and Lam Y 2001 *IEEE J. Quantum Electron.* **QE-37** 888
[15] Degnan J J, Barry D C and Richard B K 1998 *IEEE J. Quantum Electron.* **QE-34** 887
[16] Tso Y F 1988 *IEEE J. Quantum Electron.* **QE-24** 2345
[17] Riseberg L A and Moos H W 1968 *Phys. Rev.* **174** 429
[18] Palombo F K, Matthews S, Sheldrake S and Kapps D 1993 *OAS Proc. On Advanced Solid State Lasers* **15** 18
[19] Hovis F E, Stuff M, Kennedy C J and Vivian B 1992 *IEEE J. Quantum Electron.* **QE-28** 39